# P9R.7 PRELIMINARY P0LARIMETRIC ANALYSIS OF A WINTER STORM CAUSING CATASTROPHIC TRAFFIC PROBLEMS

Timo Puhakka*
University of Helsinki, Finland

## 1. INTRODUCTION*

In Finland, perhaps the most difficult road traffic problems are those caused by sudden variations in road conditions, especially in the winter season. People are accustomed to drive in all kinds of winter conditions, and are capable of this, provided that they have time to adjust to a new situation. However, in cases where conditions change rapidly and without advance information, great difficulties are to be expected.

This was the case in the early morning of the 17th of March 2005 on all major highways leading into Helsinki. After a high pressure situation lasting several days, the roads were generally clean and dry without any ice or snow, with braking conditions virtually as good as in summer. The air temperature at the surface was about -8 degrees Celsius and snowfall related to a cyclone passing Southern Finland was correctly forecasted for the area. Snowfall began at about 03 UTC and was obviously intensifying, gradually making the roads slippery.

Beginning at 05.45 UTC the situation changed dramatically. Within a 15 minute period, about 500 cars approaching Helsinki crashed on the four main highways. Three people were killed and almost 70 injured. In addition to numerous single car crashes, on all highways there were massive multiple crashes, in which dozens of cars collided at a single location. It is notable that most of the massive crashes took place almost simultaneously on all four highways at distances of 15 – 25 km from Helsinki in the north-eastern sector, as can be seen from Figure 1.

According to drivers, the conditions were slippery and got worse rapidly. Dense freezing snow mixed with supercooled water, which froze immediately on the road surfaces and on car windows, made the roads extremely slippery and the visibility so extremely poor that it was almost impossible to avoid collision with those cars ahead which had already met with difficulties. The purpose of this study is to investigate the possibilities of finding out relevant signatures related to freezing precipitation and bad road conditions, using the new University of Helsinki

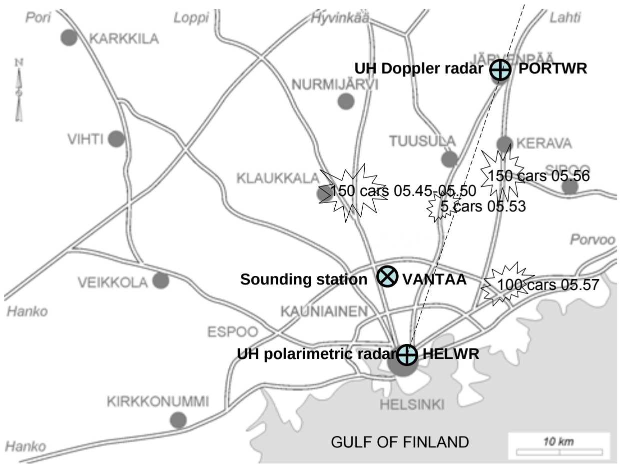


**Figure 1**. Locations and times of the massive multiple car crashes as well as the locations of the two radars and the sounding station "Vantaa". The direction of the RHI cross-sections in Figures 4, 6, 7, 8 and 9 is indicated by a dashed line.

polarimetric research radar setup, which was suitably located with respect to the region where the crashes took place (Figure 1).

## 2. RADAR SETUP

The University of Helsinki operates a mini-network of two C-band research weather radars. One of the radars (HELWR) is a new, full-coherent dual polarization radar. It has been recently built and installed in the Weather Radar Laboratory of the University, located a few kilometres north of central Helsinki. This radar transmits simultaneously horizontally and vertically polarized pulses, and also receives simultaneously the corresponding echo signals, obtaining estimates for the horizontal equivalent reflectivity factor $Z_e$, the differential reflectivity $Z_{DR}$, the specific differential phase $K_{DP}$ and the copolar correlation $\rho_{hv}$. The linear depolarization ratio LDR is estimated by switching the whole power transmitted to the horizontal channel and receiving both the horizontally and vertically-polarized signals.

* *Corresponding author address:* Timo Puhakka, Div. of Atmospheric Sciences, P.O.Box 64, FIN-00014 University of Helsinki, Finland; e-mail: timo.puhakka@helsinki.fi

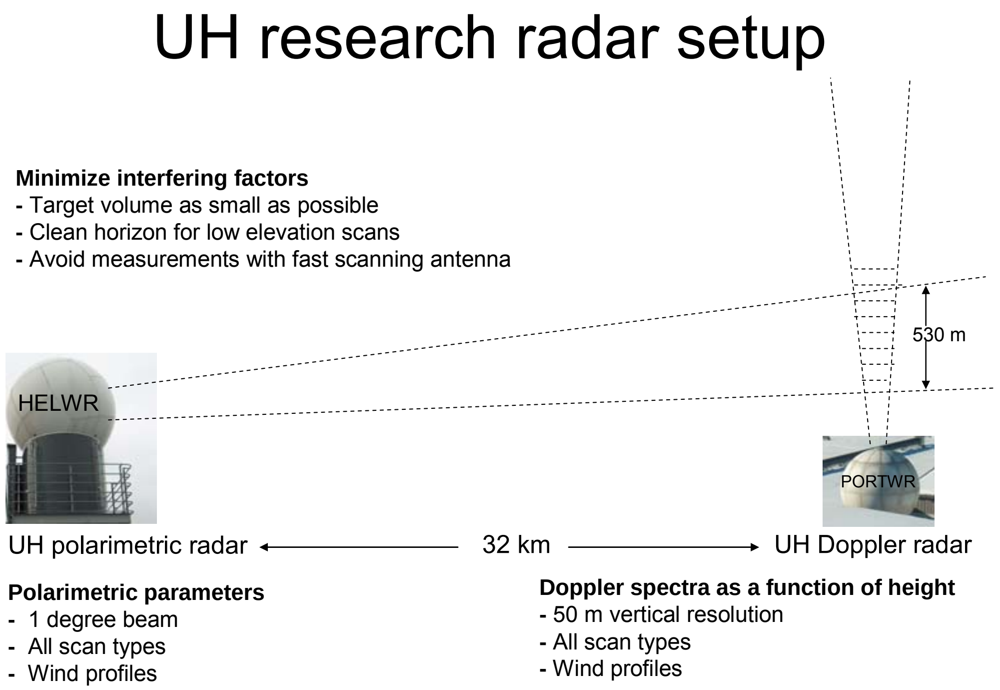


**Figure 2**. University of Helsinki Weather radar setup.

The 20-year-old single polarization C-band magnetron Doppler radar of the University is the other radar of the setup. It was recently removed from its permanent location, and made portable by installing it in a container. Although this radar (PORTWR) is old, in 1996 its receiver was upgraded to a linear digital IF receiver/signal processor. For the planned research with the new dual polarization radar, PORTWR has now been put into operation at a location 32 km north of HELWR (Figure 2).

Both radars have full scanning capabilities, but in the present setup, only the polarimetric HELWR makes both RHI-scans and volume-scans, whereas PORTWR is mainly used just pointing vertically to estimate Doppler spectra as a function of height, for use in conjunction with HELWR.

RHIs obtained by HELWR at one-minute intervals were used mainly for estimating polarimetric parameters as accurately as possible. For that reason very slow scanning speeds were used. Small PPI-volumes were recorded at 20 min intervals by HELWR to obtain a general view. The RTIs with spectra recorded by PORTWR at 10 s intervals were mainly intended to get the vertical profiles of precipitation falling speed as well as to get some idea about the particle sizes and the precipitation phase (solid or liquid) in the measurement volume of HELWR. VVPs were made regularly by HELWR and occasionally by PORTWR to get wind profiles.

Both radars were carefully calibrated in the traditional way for reflectivity measurements. However, the balance of the polarimetric channels was not yet completely calibrated at this time. This may have caused some unknown bias in the differential reflectivity and in the linear depolarization ratio.

## 3. RESULTS

### 3.1 Meso-scale and cloud-scale features

The snowstorm of March 17, 2005 was related to the precipitation band of an occluded cyclone (Figure 3). The appearance of the storm over our study area can be divided into three phases: the preceding light-snow phase (from approximately 03.00 until 05.30 UTC), the active phase (from 05.30 until 07.00 UTC), and the storm-weakening phase (from 07.00 UTC onwards). Most car accidents happened at the beginning of the active phase, between 05.45 and 6.00 UTC.

Figure 4 shows examples of the three phases as RHI snapshots of $Z_h$. The light-snow phase (Figure 4a) is characterized by a deep stratiform cloud mass extending from the surface to a height of about 7 km with values of equivalent radar reflectivity up to 15 $dBZ_e$. With time the top of the cloud mass lowered gradually to 4 km, and the highest values of the equivalent reflectivity factor increased to up to 30 $dBZ_e$ when the active phase began in our study area.

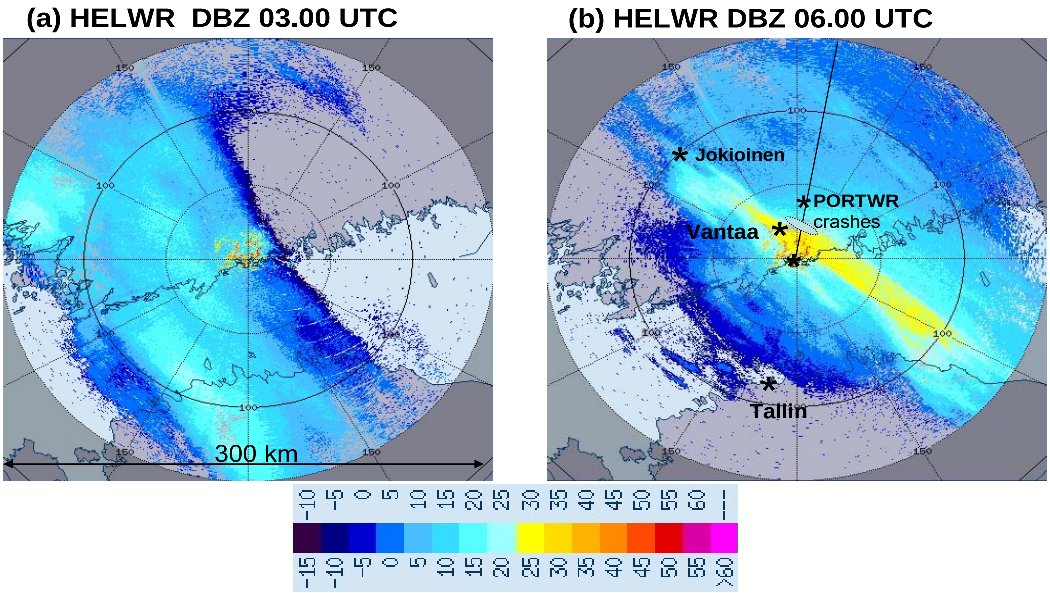


**Figure 3**. Low elevation angle reflectivity PPIs from HELWR a) 03 UTC (light-snow phase), and b) 06 UTC just after the crashes. Also indicated are the locations of the main crashes (oval), the direction of the RHI cross-section in Figures 4, 6, 7, 8 and 9 (black line), the locations of PORTWR and the sounding stations (Tallin, Vantaa, Jokioinen) referred to in the text (asterisks).

The active phase (Figures 4 b and c) is characterized by enhanced convective activity and, in general, higher absolute values and larger gradients of equivalent reflectivity. Specifically, there is a distinct horizontal band of maximum reflectivity of about 30 $dBZ_e$ entering our area from the south-west, first in the lowest 500 m layer and then extending within an hour up to a height of 2 km (Figure 4b). This band corresponds with the highest precipitation density at the ground.

Above this horizontal low-level reflectivity maximum, which moves at 8 – 9 m/s in the direction of the RHI plane, there are smaller vertical structures of enhanced reflectivity extending to near the top of the cloud mass. In Figure 4b (05.59 UTC) the first of these structures has just entered into the RHI from the left of the figure. In Figure 4c (06.27 UTC) the vertical structure is just arriving at the location of PORTWR at a distance of 32 km, while a second structure is just entering from the left. The horizontal distance between the two vertical structures is about 20 km. Initially the structures move at 9 m/s in the direction of the RHI plane, but gradually slow down, so that after 06.30 UTC their speed is only 7 m/s. At the same time the structures themselves as well as the maximum reflectivity band below them, have descended to close to the surface.

The vertical structures resemble the small cold-front-like “cold air pulses” or “cold surges” found in connection with occluded fronts (Saarikivi and Puhakka 1990). Each pulse pushes the relatively warm and moist air that is below and ahead of the pulse upwards and forwards as required by the occlusion process. On a larger scale, the underlying front is a warm front.

Between these “cold pulses”, the cloud top and the reflectivity variations below the top show remarkable convective activity compared to the preceding light-snow phase. This belt of convection resembles the generating cells found in connection with frontal precipitation bands in mid-latitude cyclones (Browning (1990), Herzegh and Hobbs (1981), Hertzman and Hobbs (1988)). According to Figure 3, the belt of generating cells and the corresponding precipitation band is oriented from south-east to north-west. This band, which is 30-40 km wide, is very likely the “upper cold frontal” precipitation band. The first “cold pulse” is located just at the leading edge of the upper cold frontal precipitation band. The reflectivity maximum

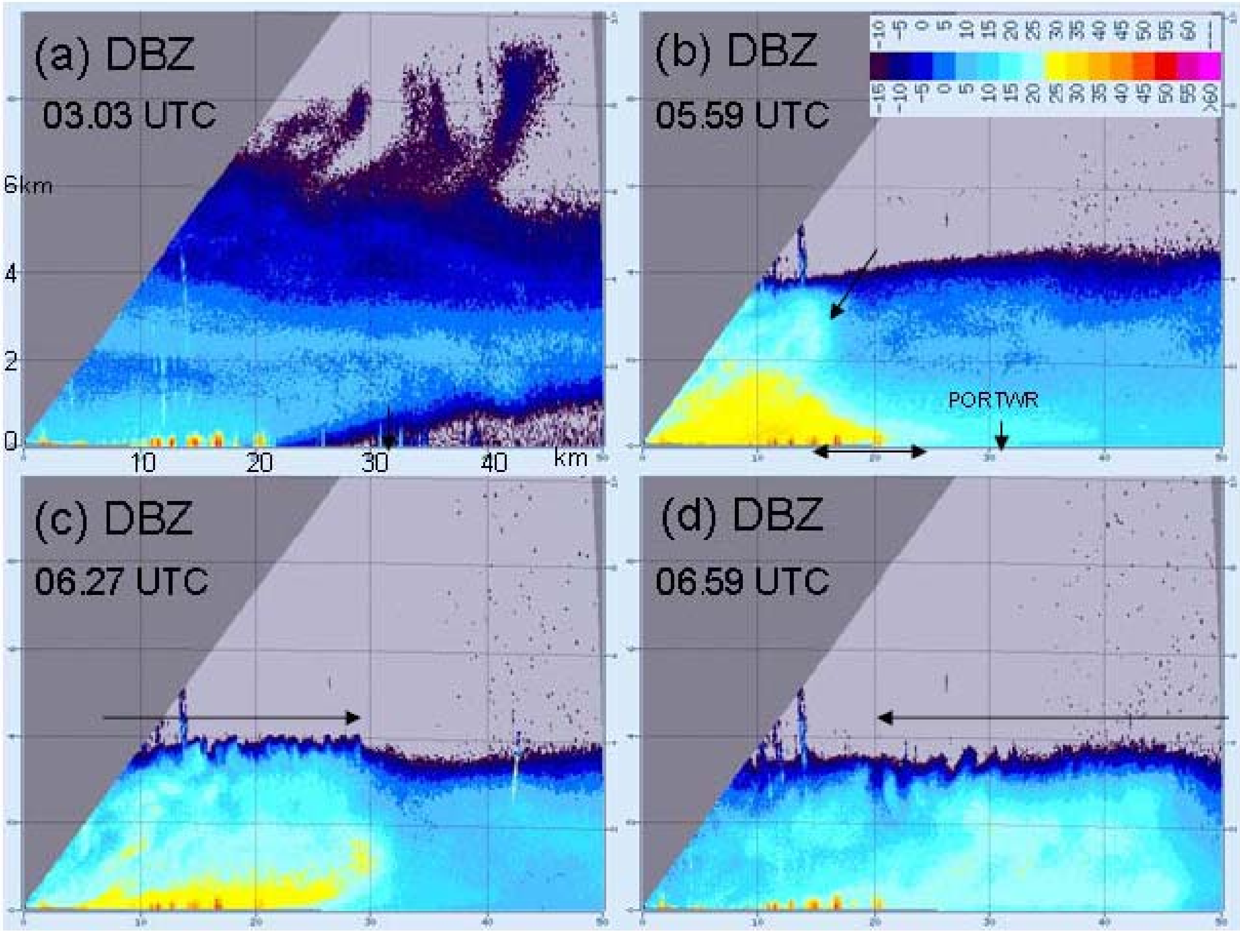


**Figure 4.** Reflectivity cross-sections from HELWR towards PORTWR on March 17, 2005 at a) 03.03 UTC (light-snow phase), b) 05.59 (beginning of active phase). Also indicated are the locations of the crashes (horizontal double arrow), PORTWR (vertical arrow) and the front of the first "cold pulse" (sloping arrow), c) 06.27 (active phase) with the horizontal extent of the area of enhanced convection indicated by the arrow, and d) 06.59 (end of the active phase).

coinciding the "cold pulse" is related to precipitation enhanced by the ascending motion at the leading edge of the upper front. The warm moist air below and ahead of the upper cold frontal band may partly be responsible for preserving existing liquid droplets, generating new droplets and ice crystals, probably melting ice-particles and eventually, causing wet snow and supercooled water.

In Figure 4d the rear edge of the upper cold frontal precipitation band has passed the radar. After the precipitation band, convective activity weakens somewhat, though this precipitation-weakening phase still contains clearly more convective activity compared with the "light-snow phase" at the beginning.

Routine radio soundings are not adequate for analysing such detailed features, but the 00 UTC soundings from Tallin and Jokioinen, and the first test soundings of the day launched from the test sounding station "Vantaa" of Vaisala Ltd (06.09 and 08.34 UTC) (see figure 3 for the locations of the soundings), give an indication that pockets of relatively warm and moist air could have existed (Figure 5). These pockets are originally due to the warm sector air (or more specifically, warm conveyor belt air) which in this case may have been moistened and heated further by the open Baltic Sea. According to the 12.00 UTC sounding from Visby (500 km SW of the radar), air temperatures at the surface were indeed about +5 degrees Celsius and the zero level was at 1500 m over the Baltic Sea. In Tallin the surface temperature was – 6 degrees with a maximum of -2 degrees within the lowest 100 m layer at 00 UTC. At 06.09 UTC the maximum at Vantaa (Figure 5) was -4$^{o}$C at a height of 0.5 km.

On the other hand, surface temperatures were clearly below zero over the study area in Southern Finland, being initially -8$^{o}$C, then increasing so that at 12 UTC the surface temperature was -4$^{o}$C before beginning to

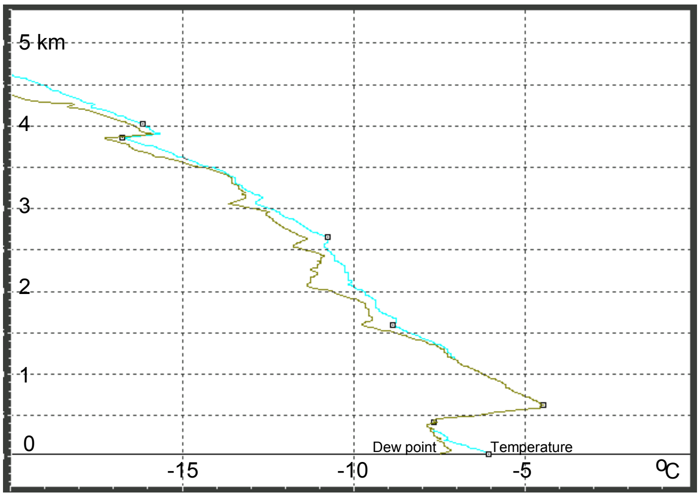


**Figure 5**. Radio sonde sounding from the “Vantaa” sounding station at 06.09 UTC 17 on Mar 2005.

fall again. Soundings indicated temperature increase with time at higher levels as well. Thus the front was a warm front type of occlusion. The existence of considerable warm advection was clearly supported by the typical wind profiles obtained both from the radio soundings, and from the radar VVP-wind profiles.

From the soundings it can be concluded that the maximum in-cloud temperatures over Southern Finland were roughly -5 degrees at a height of about 1000 m. Due to the advection, the vertical temperature structure changed gradually to become more isothermal (-5 - -8 degrees) in a 2500 m deep layer. While the humidity was high, the conditions were favourable for supercooled water. According to an aircraft observation made while making routine test measurements on the Helsinki area beacons, severe icing was indeed observed at and below the 1000 m level (Kari Tiihonen, personal communication). No information is available from higher altitudes.

### 3.2 Precipitation fall speeds

The enhanced convective activity as well as the fall speeds in the precipitation band in question can be studied more closely from the vertical measurements made byf PORTWR. Before the active phase, fall speeds were quite steady throughout the cloud layer, being close to 1 m/s. From 06.25 UTC onwards, when the upper cold frontal precipitation band arrived at the location of PORTWR, 32 km from HELWR, the situation changed. Some 15 min before the enhanced reflectivity of the first “cold pulse” arrived (06.27 UTC), the mean fall speed within the cloud layer dropped to about 0.6 m/s. This can be interpreted as an increasing positive vertical velocity of warm moist air ahead of the pulse. At and just behind the reflectivity maximum of the surge (06.28-06.33 UTC) fall speeds are higher, being on average 0.8 m/s. The variability of the velocity is also larger than before the active phase. Values exceeding 1.4 m/s are typical near the surface.

Within the upper cold frontal precipitation band the fall speeds vary even more, indicating convective variation in the vertical velocity of the air, or variation in particle sizes and types, or both. As an example, at 06.34 UTC the layer-mean fall speed is 1.1 m/s, with values higher than 1.4 m/s just above surface. Three minutes later, the mean fall speed is only 0.5 m/s with ascending motion of 0.5 m/s both at the surface and near the cloud top. After three more minutes the situation is again reversed. The enhanced convective activity ended at around 07.00 UTC at PORTWR.

### 3.3 Polarimetric signatures

There is not much of interesting in the polarimetric parameters in the light-snow phase. The patterns of $Z_h$ and $Z_{DR}$ are stratiform and relatively smooth, without large variations and horizontal gradients. Values of $Z_{DR}$ are in general smaller than 1 dB. $K_{DP}$ is diffuse and the values are close to 0 degrees/km. The LDR is typically -30 dB (where detected), and $\rho_{hv}$ is close to 1 everywhere.

The situation changes at the beginning of the active phase. This phase is characterized by enhanced convective activity and, in general, higher absolute

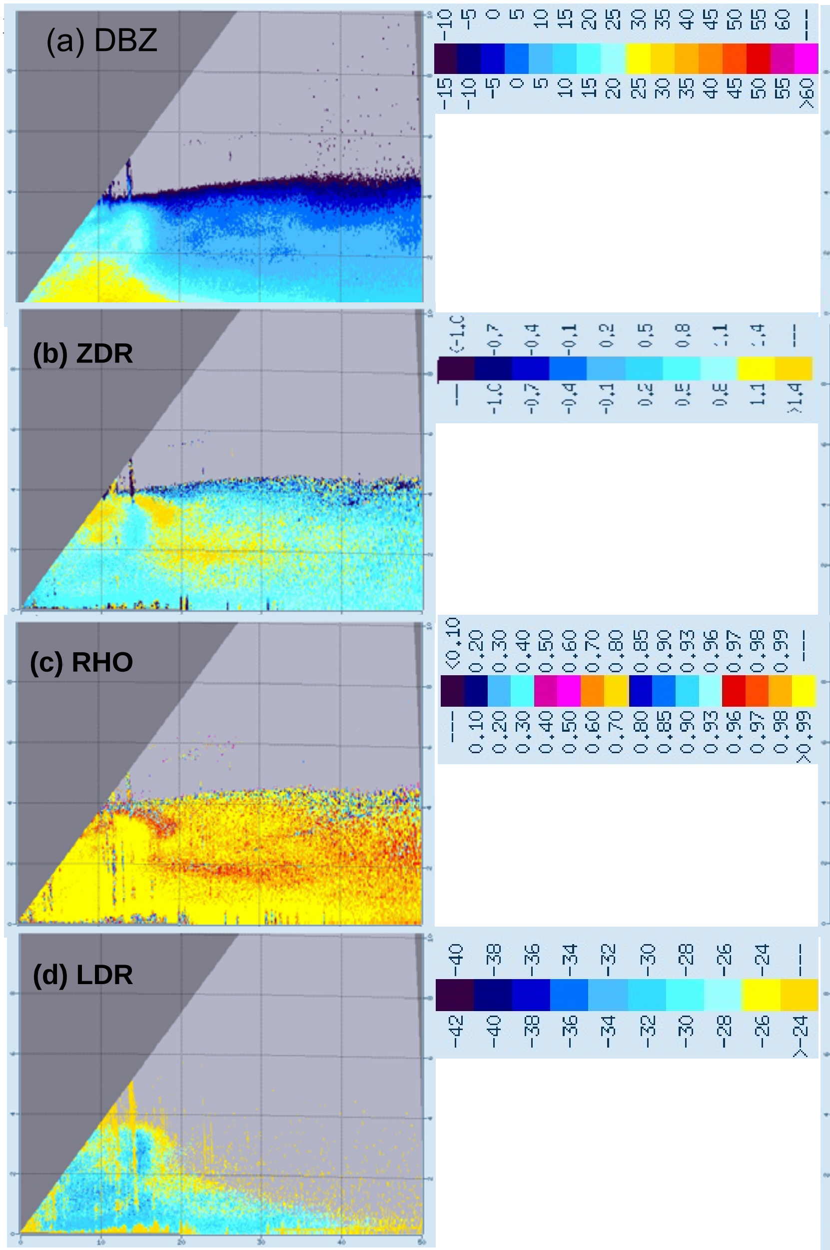


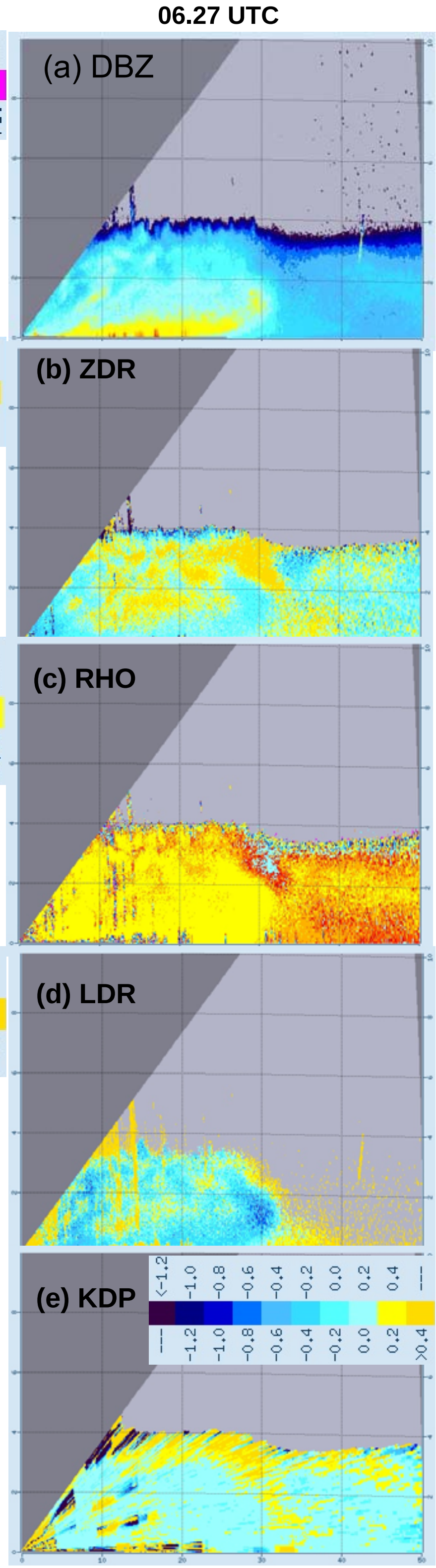


Figure 6. (above) RHI cross-sections from HELWR towards PORTWR on March 17, 2005 at 05.58 UTC a) $Z_e$ (dBZ) , b) $Z_{DR}$ (dB), c) $\rho_{hv}$, d) LDR (dB). Vertical lines at 10 km intervals, horizontal lines at 2 km intervals.

Figure 7. (right) As Figure 6 but at 06.27 UTC. e) $K_{DP}$ (degrees/km).

values and larger gradients of the equivalent reflectivity and other polarimetric parameters. Figures 6 and 7 show RHI cross-sections of polarimetric parameters at the beginning (05.59 UTC) and during (06.27 UTC) the active phase. It can be seen from the differential reflectivity RHIs (Figures 6b and 7b), that just ahead of and above the reflectivity maximum of the first "cold pulse", there is a well defined local maximum in the differential reflectivity, where values of $Z_{DR}$ higher than 3 dB are found. It should be noted that the $Z_{DR}$ maxima and the Z maxima are not co-located. At the reflectivity maximum of 25 dBZ in the "cold pulse", $Z_{DR}$ is only about 0.5 dB. According to Bader et al. (1987) and Vivekanandan et. al. (1994) this may mean a region of heavily aggregated snowflakes. At the location of the $Z_{DR}$ maximum of 3 dB in front of the "cold pulse", Z is only about 7 dBZ. According to the same authors, this is an indication of predominantly dendritic pristine ice crystals. In our case, dendritic crystals are likely, as the prevailing temperature of -15$^o$C and high humidity content are favourable for dendritic growth.

There are also one or two diffuse horizontal bands of relatively high $Z_{DR}$ values with a moderate Z: at a height of 2 km ahead of the "cold pulse", the maximum $Z_{DR}$ is about 2 dB while Z is 5-10 dBZ, and at a height of 1 km, the maximum $Z_{DR}$ is about 1.5 dB where Z is 20 dBZ. Elsewhere typical $Z_{DR}$-values are clearly below 1 dB.

In summary, the reflectivity maximum of the "cold pulse" may consist of heavily aggregated dry snowflakes while the $Z_{DR}$ maxima ahead od the "cold pulse" may contain predominantly dendritic ice crystals. According to Zeng et al. (1999), a local maximum of $Z_{DR}$ above the freezing level may also indicate the existence of supercooled water. This is further justified by the correlation, and probably also by the LDR. The lowest correlations, $\rho_{hv}$ <0.96, are found at approximately the same locations where $Z_{DR}$ has its maxima (Figures 6c,d and 7c,d). According to Vivekanandan et al (1999) and Straka et al (2000), this may be an indication of a variety of particle types. Due to the weakness of the horizontal reflectivity, LDR disappears at these locations, but a tendency towards values higher than – 24 dB can probably be recognized. Elsewhere the value of LDR is lower than -30 dB, and $\rho_{hv}$ is close to 1 (>0.98).

The distribution of $K_{DP}$ shows a diffuse local maximum belt of about 0.4 degrees/km closely correlated with the local maximum of $Z_{DR}$ at 2 km and reaching down from there to close to the ground (Figure 7e). The essential features of the polarimetric parameters related to the onset of the active phase are summarized in Figure 8.

### 3.4 Particle trajectories

Using the fall speed of the precipitation measured by PORTWR, and the wind profiles obtained from the HELWR VVP-scan at 06 UTC, approximate storm-relative particle trajectories can be constructed backward from the locations of the crashes, which took place about 20 km north of HELWR. In Figure 9 are shown 5 trajectories ending at the ground at 05.59 UTC. The trajectories were calculated using three different profiles of fall speeds, measured at 06.24, 06.25 and 06.27 UTC by PORTWR, when the enhanced maximum reflectivity of the first "cold pulse" had just arrived at the location. However, the differences in the fall speed profiles did not make any significant difference to the results.

The trajectories show that those particles reaching the ground at 05.59 UTC at the average location of the crashes, originated from three regions, where the differential reflectivity and correlation had their local maxima and minima respectively, and where also the LDR may have had its highest values. Referring to Figures 6 and 8 these regions are:

i) ahead and above the maximum reflectivity of the first "cold pulse", and
ii) two roughly horizontal layers preceding the "cold pulse" at heights of 2 km and 1 km.

These are the areas where the relatively warm and moist air is ascending. As the horizontal layers (ii) extend some 10 – 20 km or more ahead of the location of the "cold pulse", there may have been freezing precipitation, originating from these features, at the ground already well before the accidents. This is in accordance with the observations of many car drivers (including myself) that the roads were already slippery half an hour before the crashes. From Figure 7 it is also obvious that the band of slight maximum in the specific differential phase closely follows the particle trajectories from the location of the $Z_{DR}$ maximum above 2 km down to the ground.

Before coming to any conclusions, the two main assumptions made in deriving these simple storm-relative trajectories should be considered. First, it was assumed that the storm is quasi-two dimensional, and secondly, that the storm structure does not change too much during the time required for the particles to fall to the surface. From Figure 3 it can be seen that the storm is a roughly two-dimensional 100 km wide band moving NE. From Figures 6 and 7 it can be seen that the most important features of the storm, i.e. the reflectivity maximum of the "cold pulse" and the related (but not co-located) features in $Z_{DR}$, $\rho_{hv}$, LDR and $k_{DP}$ discussed above, may not have changed too much during a 30-min time-interval. The major change, which easily can be seen comparing Figures 6 and 7, is the gradual descent of 1 km by the reflectivity maximum and the related features. This process does not change the conclusions. It actually increases the time which the falling precipitation particles spent within those parts of the cloud where wet snow and super-cooled water is most probable.

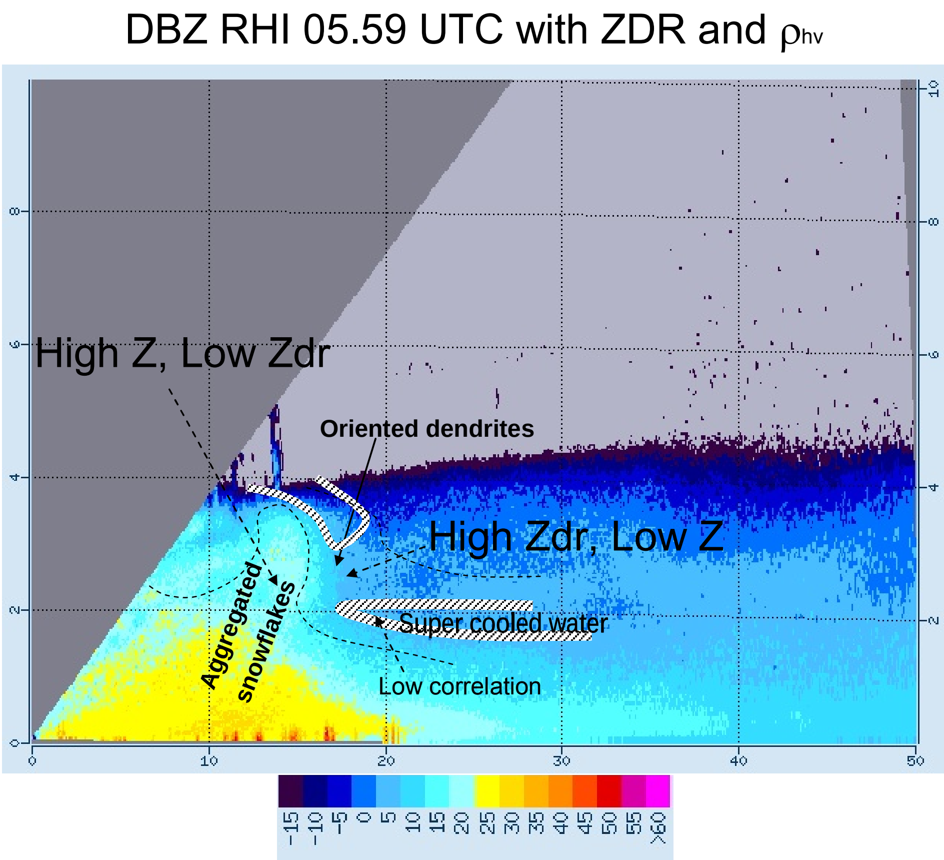


**Figure 8**. Summary of the polarimetric features at 05.59 UTC overlaid on the reflectivity cross-section.

In Figure 9 trajectories reaching the ground simultaneously at different locations relative to the storm are seen. From this figure it can be concluded that at 05.59 UTC and at locations farther than 20 km from the radar the precipitation was most likely snow with supercooled water or wet snow (red trajectories), while at closer locations (white trajectories) the precipitation was mainly dense, heavily aggregated snow. This sequence of conditions resulted in very slippery road conditions with a sudden decrease of visibility to almost zero at the locations of the crashes.

## 4. CONCLUSIONS

This very first study applying the new research radar setup of the University of Helsinki demonstrated many of the possibilities of this arrangement. We happened to be carrying out one of the first measurement trials in a winter storm causing extremely bad traffic conditions around Helsinki. During a 15 min period about 500 cars crashed, three people were killed and about 70 injured.

The storm was related to a frontal precipitation band system in an occluded cyclone. The air temperature at the ground was at all times well below zero, varying between -9 and -4 $^{o}$C. Many drivers reported freezing precipitation, supercooled rain and dense snow which limited visibility. A report of severe icing experienced by an aircraft confirmed the existence of super-cooled water.

Polarimetric RHI measurements with the coherent polarimetric C-band radar showed distinct differences peculiar to the active icing phase as compared to other parts of the storm. Before the icing phase, patterns of reflectivity and other polarimetric parameters were smooth without large variations and gradients. Low reflectivity, low differential reflectivity (< 1 dB) and high correlation values at subzero temperatures indicate light dry snowfall during this phase.

With the onset of the active phase, larger variations and gradients appear in most of the parameters. The active phase is interpreted as being a precipitation

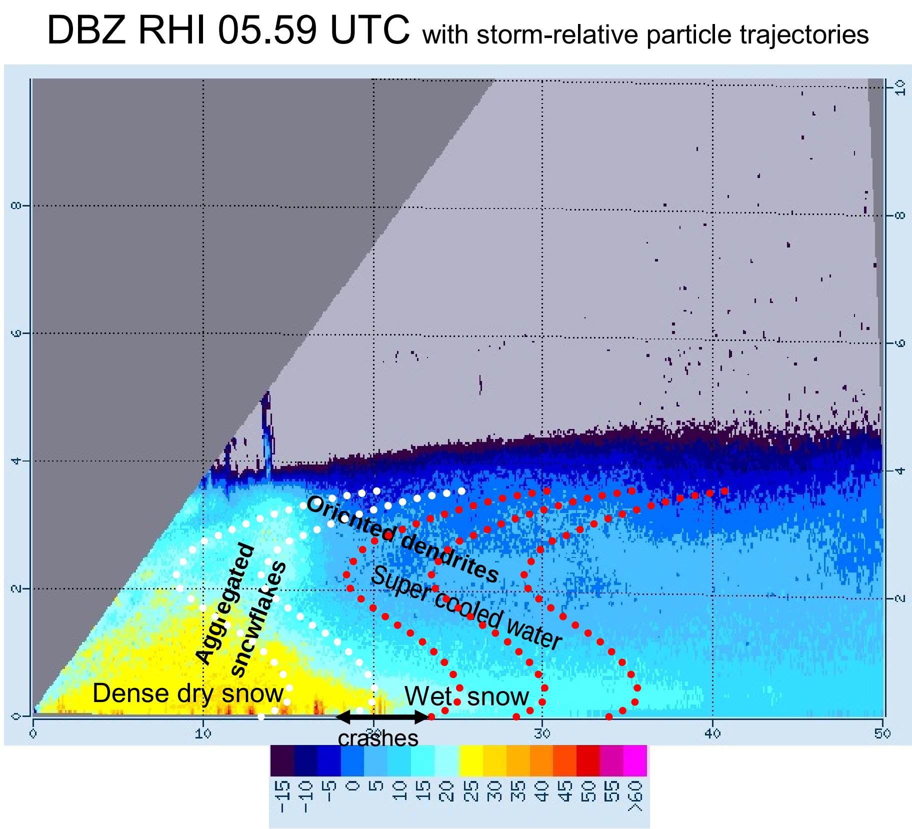


**Figure 9**. Estimated storm-relative trajectories of precipitation particles reaching the ground at 05.58 UTC, overlayed on the reflectivity cross-section at that time. Red trajectories fall through areas favourable for dendritic crystals and supercooled water. White trajectories originate and fall through regions of heavily aggregated snow.

band related to a pre-frontal cold surge. The most important polarimetric features are

1. A local, vertically-oriented maximum in the reflectivity $Z_e$ co-located with local minima of the differential reflectivity $Z_{DR}$ and the linear depolarization ratio LDR, all situated in the region of the highest correlation $\rho_{hv}$.
2. Ahead of the reflectivity maximum (1), but not co-located with it, sloping maximum bands of the differential reflectivity $Z_{DR}$ and the specific differential phase $K_{DP}$. Embedded within these features are local minima of the correlation $\rho_{hv}$.
3. In general the correlation is high at and behind the reflectivity maximum (1), while ahead of it the correlation is lower.
4. A region of enhanced convective activity behind the reflectivity maximum (1).
5. The above features descended gradually by 1 km in 30 minutes, while they moved horizontally at a speed of about 9 m/s in the direction of the RHI.

At the reflectivity maximum (>25 dBZ) (referred as 1) which assumed to be at the front edge of the cold surge, the differential reflectivity $Z_{DR}$ is close to zero, indicating heavily aggregated low density snowflakes (Bader et al 1987). This is supported further by the very low minimum value of the LDR
(< -38 dB).

In front of the reflectivity maximum (referred as 2 ) and the cold surge, the differential reflectivity has its maximum value (> 3 dB) indicating the existence of supercooled water (Zeng et al 2001) or predominantly horizontally-oriented pristine dendritic ice crystals (Vivekanandan et al 1994), or both types mixed. The decreased correlation in this region indeed supports the existence of a variety of particle types there (Vivekanandan et al 1999, Straka et al 2000).

Storm-relative particle trajectory analysis, based on the fall speed of the precipitation, storm movement vectors and wind-profiles, all measured by the radars of the setup, showed that freezing precipitation very likely originated from the regions of maximum $Z_{DR}$ and $K_{DP}$, where the correlation $\rho_{hv}$ had its minimum and $Z_e$ was relatively small. Severe icing was actually observed and reported by an aircraft on measurement flights at heights below 1 km.

Trajectory analysis also showed that during the time when most of the crashes happened, there was also a rapid change from light snow mixed with supercooled water to dense precipitation consisting of heavily aggregated dry snowflakes. As a result, the roads first became slippery due to the freezing of super-cooled water after which the visibility became extremely poor due to the dense snowfall.

Finally, the study showed clearly the effectiveness and great value of this kind of combination of two research radars in radar meteorological basic research. Although we had no extra in situ measurements in this very preliminary experiment, we were able to make quite a comprehensive analysis. We are especially impressed by the quality of the polarimetric parameters from HELWR, the capability of recording high-resolution fall speed spectra as a function of height and time from PORTWR, and the facility of getting wind profiles from both radars.

### *Acknowledgements*

The research is supported by TEKES (National Technology Agency). Special thanks are due to Leila Konkola, Matti Leskinen, Susanna Niemi and Pekka Puhakka, who assisted with the measurements, data processing and preliminary analysis.

### *References*

Browning, K. A., 1990; Organization and internal structure of synoptic and mesoscale precipitation systems in midlatitudes. Radar in Meteorology: Battan Memorial and 40th anniversary Radar Meteorological Conference, Am. Met. Soc., Boston, 433-460.

Hertzman, O., and Hobbs, P. V., 1988; The mesoscale and microscale structure and organization of clouds and precipitation in midlatitude cyclones. XIV: Three-dimensional airflow and vorticity budget of rainbands in a warm occlusion. J. Atmos. Sci. 45, 893-914.

Herzegh, P. H. and Hobbs, P. V., 1981; The mesoscale and microscale structure and organization of clouds and precipitation in midlatitude cyclones. IV: Vertical air motions and microphysical structures of prefrontal surge clouds and cold-frontal clouds. J. Atmos. Sci. 38, 1771-1784.

Saarikivi, P. and Puhakka, T., 1990; The structure and evolution of a wintertime occluded front. Tellus, 42A, 122-139.

Straka, J., Zrnic´, D., and Ryshkov, A., 2000; Bulk hydrometeor classification and quantification using polarimetric radar data: Synthesis of Relations. J. Appl. Meteorol., 39, 1341-1372.

Vivekanandan, J., N. Bringi, M. Hagen, and Meischner, P., 1994; Polarimetric radar studies of atmospheric ice particles. IEEE Trans. Geos. and Remote sensing, Vol. 32, No. 1, 1-9.

Vivekanandan, J., Zrnic´, D.S., Ellis, S.M., Oye, R., Ryshkov, A., and Straka, J., 1999; Cloud microphysical retrieval using S-band dual-polarization radar measurements. Bull. Amer. Meteor. Soc., 80, 381-388.

Zeng, Z., S. Yuter, and Houze, R., 2001; Microphysics of the rapid development of heavy convective precipitation. Monthly Weather Review, Vol. 129, No. 8, 1882-1904.